IOPscience iopscience.iop.org

Home Search Collections Journals About Contact us My IOPscience

Carrier band-to-band recombination in Mn-passivated porous silicon

This article has been downloaded from IOPscience. Please scroll down to see the full text article.

2001 J. Phys.: Condens. Matter 13 5377

(http://iopscience.iop.org/0953-8984/13/22/327)

View the table of contents for this issue, or go to the journal homepage for more

Download details:
IP Address: 171.66.16.226
The article was downloaded on 16/05/2010 at 13:28

Please note that terms and conditions apply.

INSTITUTE OF PHYSICS PUBLISHING JOURNAL OF PHYSICS: CONDENSED MATTER

J. Phys.: Condens. Matter **13** (2001) 5377–5385 www.iop.org/Journals/cm PII: S0953-8984(01)19146-0

Carrier band-to-band recombination in Mn-passivated porous silicon

Qianwang Chen[1,2], Y Zhang[1] and Y T Qian[1]

[1] Structure Research Laboratory, University of Science and Technology of China (USTC), Hefei 230026, People's Republic of China
[2] Department of Materials Science and Engineering, USTC, Hefei 230026, People's Republic of China

Received 14 November 2000

Abstract
Porous silicon (PS) was *in situ* passivated by Mn^{2+} and covered by a layer of MnO_2 using a hydrothermal technique. A 370 nm photoluminescence (PL) band, showing carrier 'band edge' recombination features, was observed, which agrees well with the inter-band transition of 3.4 eV detected by optical absorption measurements. Silicon nanocrystallites several nanometres in size were able to cause conduction band splitting; then an inter-band transition of 3.4 eV was observed due to the carrier transition between the sub-conduction band to the valence band (A1). A high potential layer of manganese oxide on the surface of the silicon nanocrystallites prevents excited carrier diffusion from the core of Si to neighbouring defects from nonradiative decay, and as a result enhances carrier band-to-band recombination, resulting in the ultraviolet PL (370 nm).

1. Introduction

Red-PL in porous silicon (PS) [1] has attracted much attention from the viewpoints of both fundamental physics and the potential application to optical devices. Currently the photoluminescence (PL) of PS covers the entire visible spectrum and extends to the IR region depending on the etching conditions and post-treatment steps [2]. Blue luminescence was found in electrochemically etched porous silicon followed by rapid-thermal-oxidation (RTO) processes [3]. It is shown that both the temperature dependence of the intensity and the decay dynamics of the blue-PL are entirely different from those of the red-PL. The blue-PL intensity decreases monotonically with increasing temperature, while an unusual temperature dependence of the red-PL intensity is observed. The initial decay of the blue-PL is approximately described by a single exponential function. The long nonexponential decay of the blue-PL is not observed, but that of the red-PL is clearly seen. These results suggest that the mechanism of the blue-PL is different from that of the red-PL, originating from the long-lived near-surface state. Several models, silicon oxide, surface state, and Si cluster [4, 5], are proposed for the origin of the blue-PL in oxidized PS. The emission from a silicon oxide model,

0953-8984/01/225377+09$30.00 © 2001 IOP Publishing Ltd Printed in the UK

widely accepted [6, 7], suggests that different types of defect in silicon oxide can be responsible for blue-PL; this idea gains support from the correlation between the intensity of the blue-PL band and the intensity of the Si–O infrared absorption. The authors also found a correlation between blue luminescence intensity and the increase in feature size caused by oxidation. They further showed that the blue luminescence is identical, with respect to the spectrum and fast decay, to that of high-microelectronic-quality SiO_2 grown on crystalline silicon using dry oxygen plus an organic chlorine compound [6, 8]. It is, therefore, suggested that the blue luminescence of oxidized PS comes from creation of oxygen-, carbon- or halogen-related defects in silicon dioxide. However, transmission electron microscopy (TEM) studies indicate that the number of nanocrystallites decreases rapidly with increasing T_{ox} ($T_{ox} > 800\,^{\circ}$C). When the number of Si crystallites decreases, the blue-PL intensity decreases. This clearly shows that Si nanocrystallites participate in the blue-PL process in oxidized PS [5, 9]. The above results lead us to believe that the photogeneration of carriers occurs in the c-Si core, whose band gap is modified by the quantum confinement effect, and the radiative recombination occurs in the silicon oxide layer. However, according to the quantum confinement model, pure band-to-band recombination could be observed. This has not been achieved due to the fact that the surface structure of Si, which is sensitive to the sample preparation and drying conditions, determines the carrier recombination process.

It is well established that the relatively clean fluorinated hydride surface of freshly etched layers is slowly converted to a contaminated native oxide during exposure to ambient air [10]. Experiments also show that the luminescent properties of PS are dependent on the way in which the material is dried after fabrication because the composition and structure of the native oxide developed can also be highly variable [11, 12]. Both ambient-air-aged and thermally oxidized PS show blue and green luminescence, for example, but the luminescent properties of these samples are quite different from each other [13]. These results clearly show that the structure configuration of the silicon oxide influences the carrier recombination process, and must be responsible for the highly variable PL properties reported. To understand well the mechanisms of radiative transitions in PS, it is very important to control its surface structure. Metal-passivation on the surface of Si crystallites has been reported by several groups [14–16]. However, a normal passivation method such as electrochemical erosion in metal ion solutions or sputtering of certain metals after erosion does not easily result in bonding of Si dangling bonds with metal ions, and the metal layer formed accelerates rather than prevents excited carrier diffusion, which makes the luminescent process more difficult to understand. Moreover, it is desirable to use more advanced structure characterization and spectroscopy measurement techniques to study the PL mechanism in PS with highly variable structure, but there appears to be no simple way to confine excited carriers in the core of c-Si, from which comparable information can be obtained for the PL mechanism study in Si-based materials as complex as PS. This paper aims to construct *in situ* a non-silicon oxide high-potential barrier layer on the surface of Si nanocrystallite to observe intrinsic PL feature of Si nanocrystallites by inhibiting excited carriers diffusion and tunnelling.

2. Experiment

For the present experiments, p-type (heavily boron-doped, 0.05 Ω cm) (001) oriented silicon wafers were fixed in the bottom of a Teflon vessel. Solutions of 0.2 mol l^{-1} HF in 1.0 mol l^{-1} $Mn(NO_3)_2$ were added to the vessel until 70% of its volume was filled; then the vessel was placed in a stainless steel tank to perform hydrothermal treatment. Most of the hydrothermal erosion was performed at 140 °C for 1 h. After the erosion process all the samples were dried in air. X-ray diffraction (XRD) was performed on a Rigaku x-ray diffractometer. X-ray

photoelectron spectroscopy (XPS) analysis was done on a VG ESCALAB MKII electron spectrometer; the basic pressure during the measurement was about 1×10^{-9} mbar. The x-ray radiation of magnesium (Mg K = 1253.6 eV) was employed as the excitation source. The PL was measured on an 850-type visible–ultraviolet spectrophotometer at room temperature, and these results were corrected for the system response. The absorption measurements were performed on an HP8452A diode array spectrophotometer.

3. Results and discussion

XRD for PS around the fundamental reflection (001) was performed. Besides a diffraction band at 69.3° for Si substrate, a broadening diffraction band around 70.2° for the PS layer was observed. The grain size of Si, calculated by Scherrer's equation, is 3 nm on average. This was further confirmed by high-resolution transmission electron microscopy (HRTEM) analysis, which reveals silicon nanocrystallites with a size of about 1–5 nm. Mn^{2+}-passivation on the surface can be viewed by XPS analysis. In the $Mn_{2p}^{1/2}$ XPS spectrum of the sample, two peaks at about 641.6 eV and 656.2 eV, respectively, were observed. This type of Mn XPS spectrum shows the co-presence of Mn^{2+} ions and MnO_2. No a-SiO_2 was detected by thin film XRD analysis. In XRD studies, x-ray 2θ-scan diffraction for Mn^{2+}-passivated PS and normal PS was carried out with θ fixed at 3°. A broadening band around 57.8° ($d = 1.62$ Å, average length of Si–O bonds) was observed in normal PS, indicating amorphous silicon oxide present in the sample, while this diffraction band was not detected in Mn^{2+}-passivated PS. These results suggest that a MnO_2 rather than an a-SiO_2 layer covered the Si nanocrystallites. However, FTIR spectroscopy shows a weak absorption band due to silicon oxyhydride (Si:O:H) near 3400 cm^{-1}. It is thus suggested that the passivated Si nanocrystallites consist of three regions: the core, interfacial and outer MnO_2 layers as shown in figure 1(A). Combining with the XPS results, it is suggested that the interfacial layer is created by co-passivation of Si dangling bonds with an OH group and a Mn^{2+} ion.

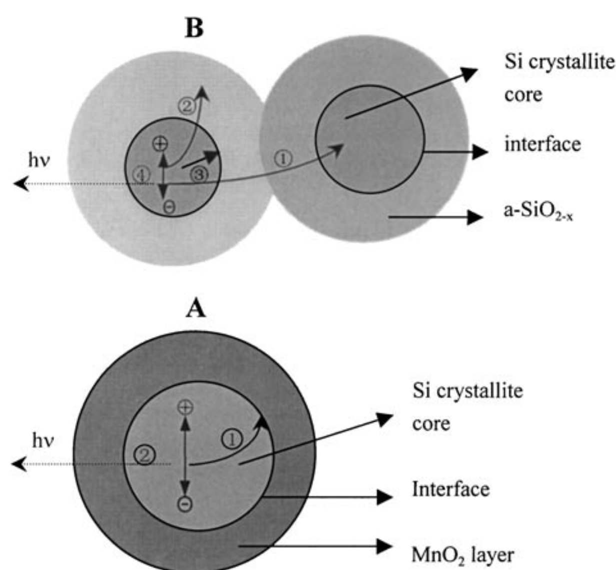

Figure 1. Schematic illustrations of excited carrier relaxation pathways in Mn^{2+}-passivated porous silicon (A) and normal porous silicon (B).

Figure 2, curve a, depicts the PL spectrum of an as-prepared Mn-passivated sample excited with 256 nm ultraviolet light. Besides the strong luminescence band around 670 nm with a lower energy component peaking at 730 nm, a strong ultraviolet PL band peaking at 370 nm was observed. The 670 nm band is broad ($\sim$0.25 eV FWHM) with Gaussian-like shape, while the 370 nm and 730 nm bands cannot be described accurately by a Gaussian distribution. In the PL spectrum of PS hydrothermally prepared at 140 °C for 1 h without addition of $Mn(NO_3)_2$, a broad luminescent band around 680 nm was observed (figure 2, curve b). By comparing the peak position and shape to that of PS without Mn^{2+}-passivation, it is suggested that the 670 nm band with the Gaussian-like shape in figure 2, curve a is the usually observed red-PL band in PS, and that the 370 nm and 730 nm bands are new PL bands possibly due to the presence of manganese.

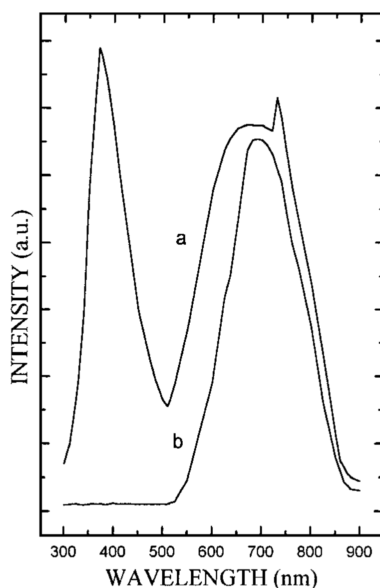

Figure 2. PL spectra of hydrothermally treated porous silicon with (curve a) and without (curve b) Mn^{2+}-passivation, excited by 256 nm ultraviolet light.

The PL spectra for PS measured by using continuously adjustable monochromatic light as excitation source show that the intensities of both of 670 nm and 730 nm bands decrease as the excitation wavelength increases. The peak wavelength remains nearly unchanged as the excitation wavelength increases (figure 3), which reflects that the two PL bands have similar luminescent origin and are not sensitive to the silicon size. According to the above three-region model, the process of radiative recombination may proceed as follows. Some of the excitons in the core are confined to the interfacial layer due to the localized states being in the c-Si gap. The 670 nm PL band is then caused by the radiative recombination of the excitons confined in the interfacial layer (Si–OH related surface state) (R2 in figure 4). The 730 nm shoulder band may also be caused by Si-Mn-related localized states or carrier transitions between the d orbit of Mn^{2+} and conduction band/or valence band. A pure d–d transition cannot be responsible for this. Typically, the Mn^{2+} ion in a semiconductor such as from the II–VI group (i.e. ZnS:Mn) introduces several levels which sometimes correlates with the crystal field splitting of Mn^{2+} ion d-levels. However, the usually observed Mn^{2+} $4T_1$–$6A_1$ transition results in a yellow emission band around 585 nm (2.12 eV) with a half width of 0.23 eV at room temperature

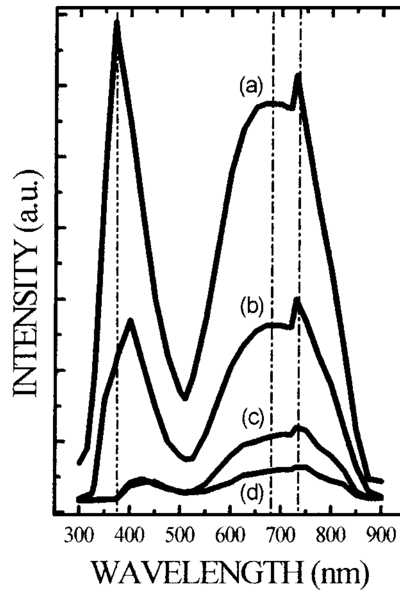

Figure 3. Room temperature wavelength and intensity dependence of PL bands on the excitation wavelength, (a) 256 nm, (b) 276 nm, (c) 296 nm and (d) 316 nm respectively.

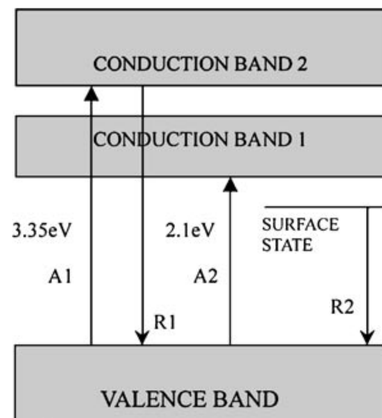

Figure 4. Schematic diagram of PS conduction band splitting structure showing the origin of optical gaps PLE and PL.

[8]. Measurement results obtained from photo- and electroluminescence show that the band gap for PS is 1.8–2.0 eV [9, 11], smaller than 2.12 eV for the Mn^{2+} $4T_1$–$6A_1$ transition. From the results reported in [8, 11], it is certain that the Mn^{2+} $4T_1$ and/or A_1 state are embedded in the conduction band and/or valence band, which suggests that the direct Mn^{2+} ion d-level transition could not be observed. Further work needs to be done to confirm this.

The band-gap energy of the c-Si core with 1–2 nm is estimated to be about 3 eV [7], which is less than that of the 370 nm (3.35 eV) PL band. In Mn^{2+}-passivated PS the strong 370 nm PL band coexists with the red-PL band, which is quite different from the feature of the blue-PL in oxidized PS. In the RTO process, at higher oxidization temperature (T_{ox}), above

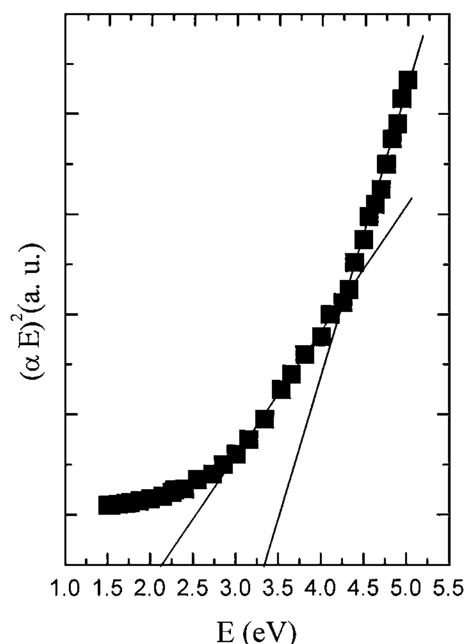

Figure 5. Plot of $(\alpha E)^2$ versus photon energy E. The energy band gap for the given sample was derived from the intercepts of the linear portions of the curve.

800 °C, a strong blue-PL near 400 nm appears, while the red-PL near 750 nm disappears [6]. FTIR spectroscopy indicates that at high T_{ox} above about 800 °C, the surface of Si crystallites is covered by amorphous SiO_2 (a-SiO_2). It is generally supposed that the blue-PL originates from the radiative recombination of carriers from the c-Si core in a-SiO_2 [5]. Figure 3 also shows that the intensity of the 370 nm PL band decreases as the excitation wavelength increases, while the emission wavelength increases, showing the quantum confinement effect. If we assign the 370 nm band in Mn^{2+}-passivated PS to the confined carrier band-to-band recombination in the core of c-Si, it is not surprising that peak position and shape change with excitation wavelength since there definitely exists a wide range of Si particle sizes, which results in a distribution of the energy gap, and increasing excitation wavelength would lead to the excitation photo energy used not being high enough to create nonequilibrium carriers across the band gap of small crystallites. To further clarify the origin of the 370 nm PL band, the optical absorption in Mn^{2+}-passivated PS was employed. In figure 5 the square of the absorption coefficient times the photon energy, $(\alpha E)^2$, is plotted versus photon energy E. The reason why the plot of $\sqrt{\alpha E}$ versus E was not used to obtain the band gap of PS from optical absorption measurements was discussed by Datta *et al*, in [17]. Two band gaps for a given sample, 3.4 eV and 2.1 eV, were derived from the intercepts of the linear portions of the curve. The 2.1 eV band gap (A2 in figure 4) agrees well with the usually determined value 9. The Si crystallites with only several crystal cells have hybrid electronic properties between the molecular and crystalline states [18, 19]; this leads us to believe that, besides the enlargement of band gap along with decreasing Si size, the splitting of the conduction band could also occur. The 3.4 eV band gap observed may be the transition between the sub-conduction band to the valence band (A1) due to conduction band splitting in Mn-passivated silicon nanocrystallites, schematically shown in figure 4. The PL excitation spectrum of

670 nm is depicted in figure 6, also shows two absorption bands. One peaks at 2.35 eV, the other band starts absorbance at about 3.3 eV and peaks at 4.7 eV, in good agreement with the results observed in (100)-oriented Si nanowires [20], which also correspond well with our absorption measurement results. Theoretical calculation also predicted that the conduction band should split for low-dimensional Si crystallite [21]; furthermore, Holmes *et al* recently found that silicon nanowires exhibited a distinct peak at 3.35 eV [20]. We can ask why, in oxidized PS, no such results were observed. In fact, higher-energy emission, such as ultraviolet emission, has often been reported in oxidized PS [22–24]. Further, optical transitions at 2.2 and 3.1–3.4 eV were also observed by electroreflectance spectroscopy [25]. We cannot rule out that it arises from the conduction band splitting of low-dimensional Si.

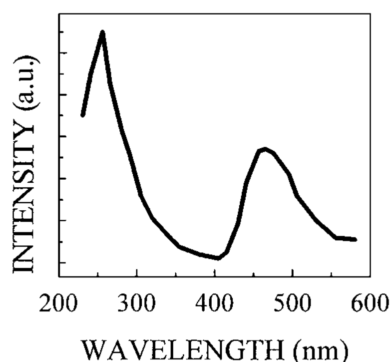

Figure 6. Photoluminescence excitation spectra of Mn^{2+}-passivated PS.

In Mn^{2+}-passivated PS, the MnO_2 layer does not itself contribute to the 370 nm band, and elimination of the origin of the 370 nm band comes from the defects in SiO_2, because the Si nanocrystallite is covered by a MnO_2 layer rather than a-SiO_2 layer. The MnO_2 layer acts as energy potential barrier to prevent carrier diffusion from the c-Si core to the neighbouring defect states for recombination. The photogenerated excitons from the c-Si core have to stay in the core; in addition, some of them are localized in the interfacial layer. The strong PL bands are then caused by the radiative recombination of excitons confined in the core and the interfacial layer, respectively. This can explain well the fact that two PL bands coexist in the PL spectrum of Mn^{2+}-passivated PS (figure 2). Figure 1(A) shows the schematic representation of the carrier relaxation pathways that can occur for the Mn^{2+}-passivated Si nanocrystallites. The excited carriers will either be localized in the interfacial region (pathway 1) or recombine to the ground state radiatively (pathway 2). We therefore suggest that the ultraviolet luminescence band comes from the carrier recombination from the sub-conduction band to ground states (R1 in figure 4). Our model can also explain well why in oxidized PS the blue-PL is not easily obtained and very sensitive to oxidation treatment [5]. In a-$SiO_{2\text{-}x}$-covered PS, the carrier relaxation pathways are schematically shown in figure 1(B). The pathways 1–3 (carrier tunnelling, diffusion into the a-$SiO_{2\text{-}x}$ layer and being confined in the interfacial region) are sensitive to the chemical environment around the Si skeleton, and tend to decrease the possibility of pathway 4, band-to-band recombination. Indeed, it has been reported that the luminescent process is determined by the structural configurations [13, 22]. The luminescence feature is strongly affected by the composition ratio of silicon–oxygen in this interfacial region and defect structure in a-SiO_2. When the transition energy of the interfacial layer is lower than that of the Si nanocrystallites, the photogeneration of excitons are localized mainly in the interfacial region, resulting in red-PL. In the case when the oxide

layer is a nonstochiometric a-SiO_{2-x}, or has defect structure, some of the excited carriers will recombine in the SiO_{2-x} layer resulting in PL or will recombine nonradiatively [26]. When the surface potential barrier is higher than that of the excited carriers, for instance, a stoichiometry a-SiO_2 forms on the Si nanocrystallites, band-to-band recombination could also occur. When the Si size is small enough to cause splitting of the conduction band, the excited carriers with higher energy diffuse more easily for nonradiative recombination or recombination in the outer oxide layer due usually to a sub-oxide layer formed between the c-Si core and the a-SiO_2 layer. That may be the reason why conduction band splitting phenomena are not easily observed in oxidized PS, and why blue–green-PL in oxidized PS is difficult to understand. For instance, it has been shown that both ambient-air-aged and thermally oxidized PS show blue and green luminescence, but the luminescent properties of these samples are quite different from each other [13]. If our model is correct, and the outside layer of silicon oxide is responsible for the different feature of blue–green-PL from group to group, researchers should observe blue–green emission in a PS sample consisting of silicon crystallites several nanometres in size without oxidation. Indeed, Von Behren *et al* has carefully measured p-Si samples kept under an argon atmosphere and never exposed to air and then observed blue emission [2]. Their experiment also further reveals that band-to-band recombination in silicon nanocrystallites could occur, otherwise no silicon oxide layer is formed that behaves as a recombination centre for diffused carriers from the silicon core.

4. Conclusions

This study shows how to confine excited carriers in the core of c-Si for observing carrier band-to-band recombination in PS. A 370 nm PL band, exhibiting carrier 'band edge' recombination behaviour, was observed in Mn^{2+}-passivated PS covered by MnO_2. A high potential barrier layer of MnO_2 prevents excited carrier diffusion rather than serving as a recombination centre, just as silicon oxide was suggested to be responsible for the enhanced carrier band-to-band recombination. It reveals that carrier diffusion and tunnelling plays an important role in the luminescent process of normal PS and must be considered in the design and manufacture of PS-based devices.

Acknowledgment

We thank the Chinese Natural Science Foundation for financial support, and the Alexander von Humbolt Foundation, Germany, for a postdoctorate opportunity.

References

[1] Canham L T 1990 *Appl. Phys. Lett.* **57** 1046
[2] Von Behven J, Tsybeskov L and Fauchet P M 1995 *Appl. Phys. Lett.* **66** 1662
[3] Petrova-Koch V, Muschik T, Kux A, Meyer B K, Koch F and Lehmann V 1992 *Appl. Phys. Lett.* **61** 943
[4] Nommura S, Zhao X, Schoenfeld O, Misawa K, Kobayashi T, Aoyagi Y and Sugano T 1994 *Solid State Commun.* **92** 665
[5] Yoshihiko Kanemitsu 1995 *Phys. Rep.* **263** 1
[6] Kontkiewicz J 1994 *Appl. Phys. Lett.* **65** 1436
[7] Chen Qianwang, Li X, Jia Y, Zhou G and Zhang Y 1997 *J. Phys.: Condens. Matter* **9** L1
[8] Tsybeskov L, Vandyshev Ju V and Fauchet P M 1994 *Phys. Rev.* B **49** 7821
[9] Kanemitsu Y, Futagi T, Matsumoto T and Mimura H 1994 *Phys. Rev.* B **49** 14732
[10] Loni A, Simons A J, Canham L T, Phillips H J and Earwaker L G 1994 *J. Appl. Phys.* **76** 2825
[11] Cullis A G, Canham L T and Calcott P D J 1997 *J. Appl. Phys.* **82** 909

[12] Canham L T and Groszek A J 1992 *J. Appl. Phys.* **72** 1558
[13] Chang S S, Sakai A and Hummel R E 1999 *Mater. Sci. Eng.* B **64** 118
[14] Halimaoui A, Campidelli Y, Badoz P A and Bensahel D 1996 *J. Appl. Phys.* **78** 3520
[15] Sailor M 1993 *Science* **261** 1567
[16] Chen C H and Chen Y F 1999 *Appl. Phys. Lett.* **75** 2560
[17] Datta S and Narasimhan K L 1999 *Phys. Rev.* B **60** 8246
[18] Ren S Y and Dow J D 1992 *Phys. Rev.* B **45** 6492
[19] Hirao M and Uda T 1994 *Surf. Sci.* **306** 87
[20] Holmes J D, Johnston K P, Doty R C and Korgel A B 2000 *Science* **287** 1471
[21] Buda F, Kohanoff J and Parrinello M 1992 *Phys. Rev. Lett.* **69** 1272
[22] Jiang D T, Coulthard I, Sham T K, Lorimer J W, Frigo S P, Feng X H and Rosenberg R A 1993 *J. Appl. Phys.* **74** 6335
[23] Lin J, Yao G G, Duan J Q and Qin G G 1996 *Solid State Commun.* **97** 221
[24] Qin G G, Lin J, Duan J Q and Yao G Q 1996 *Appl. Phys. Lett.* **69** 1689
[25] Maronchuk I, Naidenkov M, Sarikov A and Voloshina T 1999 *Tech. Phys.* **44** 122
[26] Toyama T, Kotani Y, Shimode A and Okamoto H 1999 *Appl. Phys. Lett.* **74** 3323